|| Volume 5 || Issue 8 || August 2020 || ISSN (Online) 2456-0774
INTERNATIONAL JOURNAL OF ADVANCE SCIENTIFIC RESEARCH AND ENGINEERING TRENDS

TEXTURE VARIATION IMAGE DENOISING WITH DEHAZING SPARSE TECHNIQUE

Vemula Pradeep, Merugu Priyanka

[1] *M.Tech, DECS, Eluru College Of Engineering & Technology, Eluru*

[2] *Assistant Professor ,Dept of ECE, Eluru College Of Engineering & Technology ,Eluru*

Abstract

An Image texture, as a form of particular variation, affords vital information for the human visible device. It is difficult to keep most people of photo textures, particularly the small-scale or stochastic textures which are wealthy in high-frequency variations. Current brand new denoising algorithms generally adopt a non-regional approach consisting of picture patch grouping and organization-clever denoising filtering.

While holding the versions in texture to obtain a better photo denoising, we first deceptively organization fantastically correlated photograph patches with the same kinds of texture factors through an adaptive clustering method. This adaptive clustering approach is implemented in an over-clustering- and-iterative-merging technique, wherein its noise robustness is advanced with a custom merging threshold regarding the noise level and cluster length. For texture-keeping of each cluster denoising, bear in mind that the versions in each texture are captured and wrapped in no longer most effective the among-size electricity variations but additionally the inside-size versions of PCA rework coefficients, accompanied by we suggest a PCA-transform- domain variant adaptive filtering technique to maintain the local versions in textures.

A test on images shows the conventional PCA-based totally tough or smooth threshold filtering to superiority of the proposed remodel-domain version adaptive filtering. As an entire, the proposed denoising approach achieves a commending texture-maintaining performance each quantitatively and visually, mainly for irregular textures, that is in addition verified in digital camera raw picture denoising.

Index Terms

Texture-maintaining denoising, adaptive clustering, principal component aspect evaluation transform, suboptimal Wiener filter out, LPA-ICI.

CHAPTER 1

INTRODUCTION

Digital images are common means to carry the information from or of a scene to the user in terms of visual perceptions. Image processing techniques are therefore indispensable assets to restore degradations of the information conveyed to a viewer or a computer for further analysis. There is a wide range of scientific and engineering applications that require visual information. Examples include medical diagnosis of tomography scout images and uses in remote sensing of the earth for resource exploration [1,2]..

The problem of image enhancement had been tackled with focus on the preservation or enhancement of object edges in the image [7]. A color saturation boost operation is first carried out and then rectified for edge preservation. Another method was proposed which employs a morphological filter to enhance edges for an increased sharpness on the resultant image [8].

The contrast enhancement problem was also approached adopting a block-based enhancement strategy [9,10]. These localized enhancement approaches could be more complicated in their implementations when comparing to the class of global histogram equalization methods. Image enhancement algorithms based on histogram equalization are often categorized as a statistical and global approach [11]

In addition to separating the image into high and low brightness sub-images as aforementioned, contrast enhancement could also be accomplished by modifying and specifying a target density profile in histogram equalization. For instance, the input histogram was smoothed using an intensity-based window width [22]. The strategy reported therein can be further extended to return an output image brightness which is adjusted to that of the input image. In this work, a new method is proposed to reduce the difficulties encountered in choosing a proper sub-image division threshold. First, the mean brightness of the input image is calculated. Then depending on its magnitude as compared to half of the maximum intensity, a target histogram that balances the histogram areas over the desired mean is specified. The input image is then equalized, guaranteeing a mean brightness close to the input image.

HISTOGRAM EQUALIZATION

Histogram equalization for brightness preservation While attempts had been made to restore image contrasts from Degraded sources, researchers had paid attention to drawbacks found on the histogram equalization method where the resultant mean brightness is deviated from the input image. A class of techniques to maintain the brightness was then developed. Their salient features are reviewed below.

Conventional Histogram Equalization

Let an input image be given as I={I(u, *v*)}∈ [0, L - 1], where(u,*v*) is the pixel coordinate and I(u, *v*) ∈Z is the pixel intensityor brightness ranging from 0 to L - 1. For an 8-bit digital image,L=28= 256. The image resolution is U × V width-by-height and u = 1,⋯ , U, *v*= 1, ⋯, V. A histogram is formed and then normalized to Give the probability density, from gathering the number of pixels n(i) that have intensity value i, that is [11]

$$h(i) = \frac{n(i)}{UV}.$$

A cumulative distribution function is formed from

$$c(i) = \sum_{j=0}^{i} h(j),$$

Bi-histogram Equalization

This method is based on using the input image mean intensity as threshold [17]. After the mean brightness is calculated, the pixels are then separated into the lower and higher groups or sub-images according to the mean value,

$$I_L = \{I(u,v) | I(u,v) < I_m\},$$
$$I_H = \{I(u,v) | I(u,v) \geq I_m\}.$$

Furthermore, two cumulative density functions are constructed from the two groups, that is,

$$I_{enh} = I_{L,enh} \cup I_{H,enh}.$$

The mean brightness of the output image is the averaged value of the mean brightness of the two sub-images. Note that the result may be different from the input mean brightness.

Existing Methodology

Texture, as a systematic local variation of image values, is an essential component of natural visual information reflecting the physical properties of the surrounding environment [1]. There are two basic types of texture pattern: regular texture that consists of repeated texture elements (texels) and stochastic texture without explicit texels [2], [3] Most of the real-world textures locate in-between these two extremes. Preservation of texture variation is necessary for image pre-processing tasks such as image denoising [2], [4], so as to help make better use

of natural feature details for image content interpretation. These feature-preserving image processing researches [2], [5]–[7] have attracted great attention in recent years. However, texture variation, especially the small-scale or stochastic texture variation often lies in high frequency bands. These high frequency variations are difficult to be preserved during noise removal and tend to be smoothed. The existing state-of-the-art denoising methods often adopt the nonlocal methodology [8]–[10], which firstly uses patch grouping (PG) techniques to exploit the nonlocal self-similarity (NSS) prior in natural images, and then uses denoising filters (DF) for group-wise denoising. Over-smoothness of the image textures is caused by the deficiencies in both PG and DF procedures. PG techniques collect similar (high-correlated) patches together so that DF can exploit the NSS to boost the denoising performance. During the PG process, if dissimilar patches are gathered in the same patch group, it would be much more difficult for DF to preserve the texture variations. On the other hand, applying K-means clustering to image patches can lead to heavy computational burden due to the high dimensionality of image data. To overcome these problems, an efficient adaptive clustering method is designed in AC-PT [6], which not only determines the optimal cluster number automatically, but also accelerates the clustering without dimension reduction that can lead to the information loss. However, in case of high noise level, slight under-segmentation still can be observed.

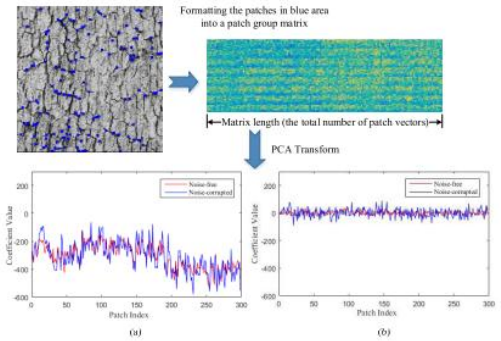

Fig. 1. The between- and within-dimension variations of PCA transform coefficients for a patch-group matrix consisting of similar patches. (a) The first dimension (signal-dominant) in PCA transform domain, (b) The last dimension (noise-dominant) in PCA transform domain. The difference between (a) and (b) shows the between-dimension variations, while the drastic fluctuation of coefficient value within (a) shows the within-dimension variations.

Noise Model

The additive white Gaussian noise (AWGN) is written as:

$y = x + n$, (1)

where x is noise-free data, y is noisy, and n follows the normal distribution with zero mean and variance σ2. AWGN is signalindependent. Being different from AWGN, the Poisson-Gaussian noise corrupting the camera raw images that are acquired from digital cameras is typically signal-dependent noise. Let x be a noise-free signal at the position c. The observed data with Poisson-Gaussian noise can be written as:

$y(c) = \rho/\alpha + bv$, (2)

$$f(y) = \begin{cases} 2\sqrt{y' + \frac{3}{8} + \sigma'^2}, & y' > -\frac{3}{8} - \sigma'^2 \\ 0, & y' \le -\frac{3}{8} - \sigma'^2 \end{cases} \quad (3)$$

where $y' = \alpha y$ and $\sigma' = \alpha b$.

Let x be the noise-free data, and the denoised data is treated as E[f (y)|x]. The exact unbiased inverse of the GAT is defined as:

$$T^{(IGAT)} : E[f(y)|x] \longmapsto E[y|x], \quad (4)$$

where $E[y|x] = x$, $E[f(y)|x] = 2\sum_{v=0}^{+\infty}\left(\sqrt{y+\frac{3}{8}} \cdot \frac{x^v e^{-x}}{v!}\right)$.

Given an image ∈ Rs×t , the total number of all the possible d × d overlapping patches Pi ∈ Rd×d is L = (s − d + 1) × (t − d + 1) with i ∈ {1, 2,⋯ , L}. The observation vector yi ∈ RM×1 with M = d2 is constructed by stretching the patch Pi . So the image can be represented as Y ∈ RM×L with each column being a stretched patch. A certain cluster can be represented with

a matrix with each column representing a stretched patch. For any data matrix Y, we add the subscript c to denote the centralized matrix Yc = Y − E(Y), where E(·) represents the expectation.. For Poisson-Gaussian denoising, we can estimate the noise parameters as in [26] and then transform Poisson-Gaussian noise into additive white Gaussian noise with unitary variance. In the following part of this paper, we focus on illustrating the novel part of the proposed denoising algorithm (in the dashed red boxes): (1) improved adaptive patch clustering for PG is discussed in Section III; (2) variation-adaptive filtering in PCA transform domain for DF is studied in Section IV; (3) sliding window and aggregation technique are discussed in Section V.

AC-STEP: ADAPTIVE CLUSTERING OF PATCHES

Many popular clustering algorithms have a common deficiency that an optimal number of clusters is difficult to be determined. However, it is easy for us to estimate an approximate range of the cluster number. Supposing the patch size is d × d and the image size is s × t, in most cases, the maximal cluster number should be below st d2 . Assuming each pixel to be the center of an image patch, we can obtain the maximal cluster number by separating the image into small non-overlapping segments, and each small segment with area approximately equal to d2 represents a distinct cluster. Meanwhile, the minimal cluster number is 1. Since we have the approximate range of cluster number (i.e., from 1 to st d2), an intuitive idea is that we can determine the optimal number of clusters by first obtaining the maximal number of clusters, and then iteratively merging the similar clusters according to a custom threshold. To this end, there are two problems that need to be solved: a) clustering a huge number of clusters requires a huge computational burden due to the high dimensionality of image patches; b) finding a way to calculate a suitable merging threshold for merging similar clusters. For the first problem, we adopt the divide and conquer technique [28], [29]. These two clusters obtained from K-means with such huge discrepancies in size usually have a very low probability of belonging to the same feature..

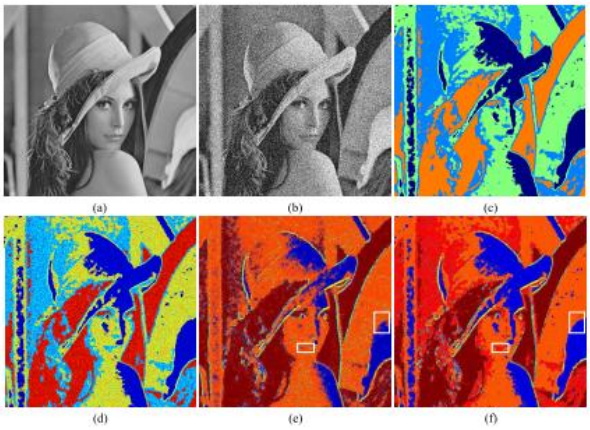

Fig. 3. The segmentation results on the noisy image with σ = 50 using K-means clustering and the adaptive clustering methods. (a) Lena; (b) Noisy image; (c) The clustering result of the first stage based on K-means; (d) Over-clustering based on divide-and-conquer technique; (e) Adaptive clustering as in AC-PT [6]; (f) Adaptive clustering considering cluster size.

Specifically, when the size of the smaller cluster in a pair of clusters is larger than a certain value LT , we decrease the probability of merging the different clusters by amplifying the between-cluster distance with an amplification coefficient ρ: Dˆ(B, A)2 = D(B, A)2/ρ. We empirically set LT = 200 and ρ = 0.7 to get a satisfactory performance.

IV. A-Step:Variation-Adaptive Filtering In Pca Domain

In PCA transform domain, inspired by the between dimension energy variations and the within-dimension variations of PCA coefficients in the signal dominant dimensions with the highest eigen values (see Fig. 1), we use a two-step texture variation adaptive approximation strategy to achieve a texture-preserving denoising performance. First, a low rank approximation is implemented via dimension selection based on hard thresholding of eigen

values to selectively preserve the energy variations of the signal dominant dimensions. Second, each signal dominant dimension is further denoised adaptively via a coefficient-wise adaptive filter with locally estimated filter parameters to protect the underlying within-dimension texture variations.

A. Dimension Selection Considering the Between-Dimension Energy Variations

Since the texture information is hardly remained in the noise-dominant dimensions with the lowest eigen values, we discard the noise-dominant dimensions via dimension selection before the within-dimension filtering to reduce the computational cost and improve the denoising performance. Considering the centralized noisy cluster matrix Yc = (yc) ∈ RM×L , Yc = Xc + N, where Xc = (xc) ∈ RM×L is noise-free and N = (n) ∈ RM×L is the noise matrix with each column vector ni ∼ NM (0, σ2I), where I is identity matrix. Suppose Yc = √L min(M,L) i=1 √λiuy,ivT y,i and the low rank approximation (with rank R) Xc = √L Rand singular vectors uy,i ,vy,i, ux,i and vx,i, 1 ≤ i ≤ min(M, L).

B. Within-Dimension Variation Adaptive Filtering

Consider the low-rank matrix YR = URPR obtained in the previous section, where UR consists of the selected eigenvectors UR = [uy,1, uy,2,⋯ , uy,R], and PR consists of the corresponding signal-dominant dimensions in PCA transform domain: PR = [p1, p2,⋯ , pR] T , (9) where pi = √Lλi vy,i (1 ≤ i ≤ R) is the selected PCA dimension. For illustrative purpose, we further extract the coefficients in any dimension pi = [pi,1, pi,2,⋯ , pi,L] and denote these coefficients in the ith dimension as the noisy observations of a "signal sequence" containing L observation points: y(n) = pi,n, n = 1, 2,⋯ , L. Let y(n) = f (n) + w(n), where w(n) is i.d.d Gaussian noise of zero mean and variance σ2 w = σ2, and f (n) (with variance σ2 f) is the noise-free signal that we want to estimate.

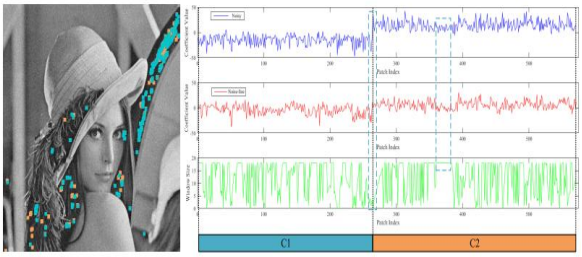

Fig. 4. Window-size determination based on the LPA-ICI method. A large patch cluster is built by the AC method from the noisy Lena image with σ = 10.

Extension

With the advances of remote sensing technology, the very high resolution (VHR) satellite and aerial images have been providing remote sensing images (RSIs) of increasing high spatial resolution, stable geometric location and detailed textural information. Two fundamental researches, scene-level geographic image classification and geospatial object detection [7], have gotten many attentions. However, these two tasks, including image analysis and search often suffer from poor quality of optical RSIs due to contrast degradation and color attenuation.

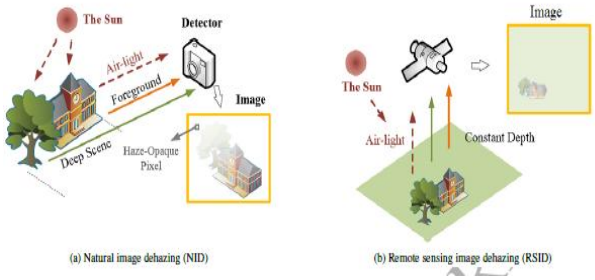

Figure 1: Physical models of natural image dehazing and remote sensing image dehazing.

To improve the quality of RSI, RSI enhancement has been extensively studied, including histogram equalization [1], homographic filter and Retinex theory [19] methods. However, this enhancement ignored the physical mechanism of haze so that it cannot remove haze adequately, usually suffering from over-saturation and gradient reversal artifacts. In fact, haze increases exponentially along with the

optical distances from scene objects to the sensor for RSIs. Hence, it is highly desirable to explore physical mechanism of haze for developing models for RSI dehazing (RSID) [23, 38]. Accordingly, the hazes usually have variety in RSIs. Thus, NID methods designed for a simple case cannot efficiently remove the hazes of RSIs. These three differences compromise the efficiency of a NID as it is applied to RSID. Although some NID models have been applied to RSID [24], the three differences should be well addressed for reaching their full potential. More recently, learning based dehazing has been developed extensively [6, 21].

Recently, a bunch of deep learning based dehazings have been developed, such as DHNet [6], MS-CNN, AOD-Net [20] and Ranking-CNN. They directly learn transmission maps on given databases.

Haze physical model for remote sensing image

A RSI is captured by the camera aboard satellite where the camera points downward the ground, so it commonly has no haze-opaque region. The bright pixels commonly belong to the reflect light of objects' surface, which cannot be used to calculate atmospheric light..

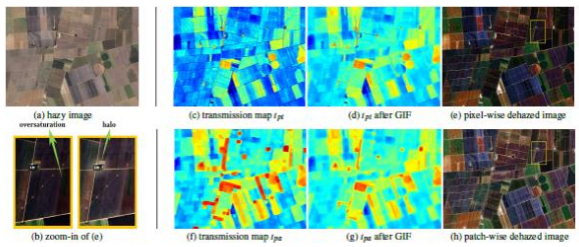

Figure 2: Comparison of pixel-wise and patch-wise dehazing.

Iterative Dehazing for Remote Sensing image (IDeRS)

Based on the discussion about transmission map estimation and atmospheric light estimation in Section 3, the IDeRS are presented in detail in this section.

Raw transmission map estimation using DCP

It cannot process RSIs efficiently since RSIs have a very large range of spatial resolution, object scale and object shape. For RSIs, a multi-scale model is more expected. Usually, the small patch size is better for high texture region, while the large patch size is better for smooth region. This phenomenon is also known as the ambiguity problem between pixel-wise and patch-wise dehazings. While, in the patch-wise output as shown in Fig.2 (f)-(h), undesirable halos near object's edges are produced. More observations reveal that halos are mostly around the region of abrupt grayscale change. We name this region Transmission Misestimated Region (TMR) where transmission is misestimated by patch-wise of (7). Therefore, pixel-wise and patch-wise models have their pros and cons. A compromise between them is desirable for optimization. For this purpose, we propose a fusion model combing pixel-wise and patch-wise dehazing models as follows.

Fusion of pixel-wise and patch-wise transmission maps

We draw a sketch map for explaining how to fuse pixel-wise and patch-wise models in Fig.3. In Fig.3 (a), a TMR is labelled by dashed curves. The abrupt gray scale occurs inside the TMR, which causes mis-estimated transmission

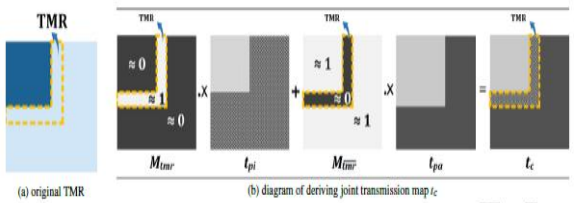

Figure 3: Sketch map of transmission misestimated region (TMR).

map using patch-wise dehazing. The fusion model can be given by $t_c(x) = M_{tmr}(x) \cdot t_{pi}(x) + M_{tmr}(x) \cdot t_{pa}(x)$, (8) where Mtmr and Mtmr respectively represent the weight maps for tpi and tpa, $0 < t_c(x) < 1$, $M_{tmr}(x) + M_{tmr}(x) = 1$, and $M_{tmr}(x) \approx 1$ for $x \in$ T MR, while $M_{tmr}(x) \approx 0$ for $x <$ T MR. For using (8), TMR should be decided beforehand, which will be discussed as follows.

Revalution and analysis

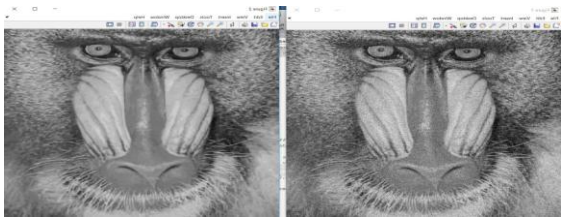

Image: 11.png (789x793), sigma: 25.0

BASIC ESTIMATE, PSNR: 29.66 dB

FINAL ESTIMATE (total time: 11.9 sec),

PSNR: 30.34 dB

ans = 30.3417

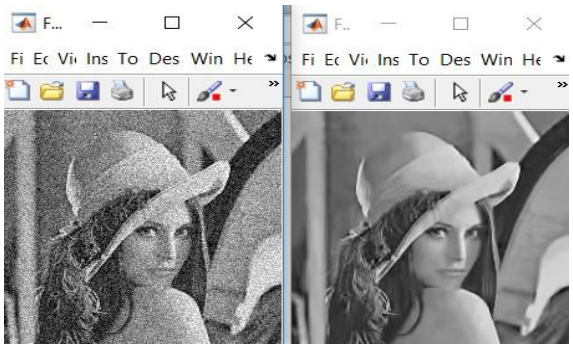

Image: l.png (225x225), sigma: 25.0

BASIC ESTIMATE, PSNR: 28.74 dB

FINAL ESTIMATE (total time: 0.6 sec),

PSNR: 29.18 dB

ans = 29.1844

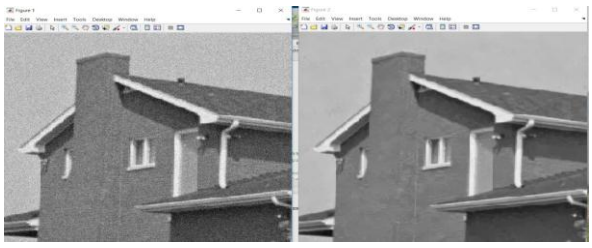

Image: 33.png (787x794), sigma: 25.0

BASIC ESTIMATE, PSNR: 34.44 dB

FINAL ESTIMATE (total time: 10.4 sec),

PSNR: 35.43 dB

ans =35.4286

Hazy images synthesized from physical haze model of (1) given t and A. Since the database does not contain heterogeneous hazy images, these two models are not good at dehazing heterogeneous hazes as illustrated in Fig.9 (g) and (h). Fig.10 shows the experimental results on suburban RSIs. This image contains farmlands, rivers, roads and small villages. Different from the high reflection of atmospheric light over building surface in urban region, the relative low reflectivity of farmland usually has similar color blocks at adjacent areas. As illustrated in Fig.10 (b), the IDeRS can obtain satisfied result on this kind of image while other methods are not quite compelling. The dehazed image by GDCP [15] shown in Fig.10 (c) has quite low contrast which cannot clearly identify the farmland blocks. Although the result of BCCR [28] and CAP [49] have more contrast than GDCP [15], their atmospheric lights are misestimated, and look quit dim. Both NLD [3] and DHNet [6] show over-enhanced, where there exist absolute black pixels (labelled

CONCLUSIONS

In this paper, we have proposed a texture-preserving nonlocal denoising algorithm ACVA. In ACVA, an adaptive clustering method is designed to adaptively and robustly cluster similar patches. A state-of-the-art PCA-based denoising filter is proposed in a transform-domain texture variation adaptive filtering approach to perform a texture-preserving denoising of each cluster. The denoising performance of ACVA is further improved via a sliding window and aggregation approach. When compared with the existing PG techniques (especially the adaptive clustering method in AC-PT), the proposed adaptive clustering method achieves more robust performance at the high noise level. In this paper, an iterative dehazing method for single RSI (IDeRS) is proposed. Firstly, we examine feasibilities of general haze optical models and dehazing algorithms for the RSID. Regarding optical model, the RSID is different from the NID in that it has almost constant depth, and without haze-opaque pixel. These two differences would lead to the failures of transmission map estimation and atmospheric light estimation,

respectively. To address the first problem, a term of "virtual depth" is defined for measuring covering and contaminant of the earth's surface, which works as the real depth of a natural image. The second problem is solved by referring to the haze-line prior [4] without the help of haze-opaque pixel. Secondly, to overcome over-saturation and halo caused by pixel-wise and patch-wise dehazings respectively, a fusion model is proposed for combining pixel-wise and patch-wise transmission map estimations. Thirdly, an iterative procedure is developed to implement transmission map estimation and whole process of dehazing. Last, evaluations on a wide variety of RSIs downloaded from NASA Earth Observatory website and five well-known databases, prove that the proposed IDeRS can better recover high quality images by gradually removing halo artifact during iterative process, at the same time, suppressing over-saturation.

REFERENCES

[1] Y. Zheng, M.P. Wachowiak, A.S. Elmaghraby, Resolution improvement anddetail enhancement for computed tomography scout images, J. Electron. Imaging14 (1) (2005) 013003.

[2] G. Zhang, X. Jia, N.M. Kwok, Super pixel based remote sensing image classificationwith histogram descriptors on spectral and spatial data, in: 2012 IEEEInternational Geoscience and Remote Sensing Symposium (IGARSS), 2012, pp.4335–4338.

[3] T. Wu, H. Wu, Y. Du, N. Kwok, Z. Peng, Imaged wear debris separation for onlinemonitoring using gray level and integrated morphological features, Wear316 (1–2) (2014) 19–29.

[4] J. Zhao, Y. Chen, H. Feng, Z. Xu, Q. Li, Fast image enhancement using multi-scalesaliencyextraction in infrared imagery, Optik 125 (2014) 4039–4042.

[5]F. Su, G. Fang, N.M. Kwok, Adaptive colour feature identification in imagefor object tracking, Math. Probl. Eng. (2012), http://dx.doi.org/10.1155/2012/509597, article ID 509597,18 pp.

[6] Y.-H. Yu, N.M. Kwok, Q.P. Ha, Color tracking for multiple robot controlusing a system-on-programmable-chip, Autom. Constr. 20 (6) (2011)669–676.

[7] K.-L. Chung, W.-J. Yang, W.-M. Yan, Efficient edge-preserving algorithm forcolor contrast enhancement with application to color image segmentation, J.Vis. Commun. Image Represent. 19 (5) (2008) 299–310.

[8] T.A. Mahmoud, S. Marshall, Edge-detected guided morphological filter forimage sharpening, EURASIP J. Image Video Process. 2008 (2008).

[9] J.-Y. Kim, L.-S. Kim, S.-H. Hwang, An advanced contrast enhancement using partiallyoverlappedsub-block histogram equalization, IEEE Trans. Circuits Syst.Video Technol. 11 (4) (2001) 475–484.

[10] N.S.P. Kong, H.Ibrahim, Multiple layers block overlapped histogram equalizationfor local content emphasis, Comput. Electr. Eng. 37 (5) (2011)631–643.

[11] R.C. Gonzalez, R.E. Woods, Digital Image Processing, 3rd ed., Prentice-Hall, Inc.,Upper Saddle River,NJ, USA,2006.

[12] L. Lu, Y. Zhou, K. Panetta, S. Agaian, Comparative study of histogram equalizationalgorithms for image enhancement,in: SPIEDefense, Security, and Sensing,International Society for Optics and Photonics, 2010, p. 770811.

[13] B.-W. Yoon, W.-J. Song, Image contrast enhancement based on the generalizedhistogram, J. Electron. Imaging 16 (3) (2007) 033005.

[14] J.A. Stark, Adaptive image contrast enhancement using generalizationsofhistogram equalization,IEEE Trans.Image Process. 9 (5) (2000)889–896.

[15] S. Poddar, S. Tewary, D. Sharma, V. Karar, A. Ghosh, S.K. Pal, Non-parametricmodified histogram equalisation for contrast

enhancement, IET Image Process.7(7) (2013)641–652.

[16]C. Wang, J. Peng, Z. Ye, Flattest histogram specification with accurate brightnesspreservation, IET Image Process. 2 (5) (2008) 249–262.

[17] Y.-T. Kim, Contrast enhancement using brightness preserving bi-histogramequalization, IEEE Trans. Consum. Electron. 43 (1) (1997) 1–8.

[18] C.H. Ooi, N.A.M. Isa, Adaptive contrast enhancement methods with brightness preserving, IEEE Trans. Consum. Electron. 56 (4) (2010) 2543–2551.

[19] C. Zuo, Q. Chen, X. Sui, Range limited bi-histogram equalization for image contrastenhancement,Optik 124 (5) (2013) 425–431.

[20] J.R. Tang, N.A.M. Isa, Adaptive image enhancement based on bi-histogramequalization with a clipping limit, Comput. Electr. Eng. (2014), http://dx.doi.org/10.1016/j.compeleceng.2014.05.017.